Journal of the Korean Chemical Society
2019, *Vol. 63, No. 1*
Printed in the Republic of Korea
https://doi.org/10.5012/jkcs.2019.63.1.12

Liquid-Liquid Equilibrium and Physical Properties of Aqueous Mixtures of Poly (Ethylene Glycol) 3000 with Tri-Potassium Citrate at Different pH: Experiment, Correlation and Thermodynamic Modeling

Mahnam Ketabi[†], Mohsen Pirdashti[†,*], and Poorya Mobalegholeslam[‡]

[†]*Chemical Engineering Department, Faculty of Engineering, Shomal University, PO Box 731, Amol, Mazandaran, Iran.*
[*]*E-mail: pirdashti@yahoo.com*
[‡]*Young Researchers and Elite Club, Babol branch, Islamic Azad University, Babol, Iran.*
(Received August 26, 2018; Accepted November 26, 2018)

ABSTRACT. The new experimental data of liquid-liquid equilibrium (LLE) of aqueous two-phase system (ATPS) consisting of poly(ethylene glycol) 3000 + tri-potassium citrate at different pH were presented. It was found that an increase in pH resulted in the expansion of the two-phase region. The TLL and STL increased with increasing the pH values. The Merchuk equation can be appropriately employed to correlate the binodal curves and also the tie-line compositions were adjusted to both the Othmer-Tobias and Bancroft equations. In order to calculate the compositions of the phase and the ends of the tie-lines, density and refractive indices as two physical properties were used. Finally, the extended UNIQUAC, UNIFAC, Virial-(Mobalegholeslam & Bakhshi) and modified UNIQUAC-FV were used to measure the phase equilibria at different pH. The results of the models suggested that it can be used quite well to correlate the LLE in an aqueous solution of polymer–salt.

Key words: Liquid-liquid equilibrium data, Density, Poly(ethylene glycol), Tri-potassium citrate, UNIQUAC-FV

INTRODUCTION

Albertsson reported the Liquid–Liquid Equilibria (LLE) of the Aqueous Two-Phase Systems (ATPSs), which included two distinct types of polymers or a polymer and a salt.[1] ATPSs are one of the most frequently applied methods especially for the protein purification in the downstream process.[1] According to the recent findings, citrates can be used instead of the inorganic salts and the sodium and potassium citrates establish ATPSs with Poly(ethylene glycol) (PEG) that works effectively for the protein extraction.[2] Moreover, citrate is favored because of some positive features such as being biodegradable and nontoxic and without any hazardous effect on the plants.[2,3] Zafarani-Moattar and Hosseinpour-Hashemi[4] obtained the equilibrium data for PEG 2000+ tri-potassium citrate + H_2O system at T = (298.15, 303.15, 308.15, and 318.15) K through the experiment. Moreover, they investigated the effect of temperature on the binodal and tie-lines for the studied system (ATPS).[4] On the other side, Zafarani-Moattar and Hamidi,[5] measured the LLE data of PEG 6000 + tri- potassium citrate + water at 298.15, 303.15, and 308 K, and found that the increase in temperature was followed by increased slope of tie-lines and the expansion of the two-phase area. Jayapal et al.[6] determined three levels of temperature (25, 35, and 45) °C for liquid-liquid equilibrium in the ATPS that included poly(ethylene glycol) 2000 + potassiumcitrate + water. Based on their findings, there was an negative correlation between the temperature increase and the downward curve change in binodal.[6] Moreover, Jayapal et al.[6] reported that the increment of solubility resulted in such negative relationship and finally this behavior may lead increment of phaseregion. Most of the studies in this regard were related to the investigation of the temperature changes on ATPS.

In our previous work,[7] the study investigated the binodal curve for PEG 3000+ tri-sodium citrate at 298.15 K and different pH (6.1, 7.5, and 9.0) and it indicated that the increase in pH resulted in the expansion of the two-phase region and an increase in the concentration of PEG 3000 in the PEG-rich phase for this system.

The thermodynamic models include three main groups namely the lattice theory, local composition and multi-model theory (combination of models), Lattice theory is the first group of thermodynamic models describing the ATPSs, in that the molecules are located in a rectangular room called the lattice, The interaction of the neighboring molecules provided the opportunity to obtain the enthalpy of mixing of the molecules.[8] The second group of the model is the local composition describing the ATPSs. Wilson,[9] NRTL[10] and UNIQUAC[11–20] are the leading members of the second group of thermodynamic models. However, the recent

studies aimed at providing more sophisticated versions of the prior models with precious measurement including MNRTL-NRF,[12] UNIQUAC-NRF,[13] and the modified Wilson.[14,15] Finally, the last group of thermodynamic models is a combination of various theories employed to obtain the phase behavior of ATPS with regard to the virial osmotic theory of McMillan and Mayer,[15] the Hill theory,[17] the solution the VERS model,[18] and extension of the Pitzer model.[19–22]

In the present work, the binodal and LLE data for PEG 3000+ tri- potassium citrate + water in three pH values (8.33, 9.60, and 10.52) were measured and correlated with model equations. Then, the composition of each phase was calculated using four thermodynamic models (extended UNIQUAC, UNIFAC, Virial-(Mobalegholeslam & Bakhshi) and modified UNIQUAC-FV. Accordingly, the findings of the results based on the experimental data indicated that this modified model correlated well with the LLE in the systems.

EXPERIMENTAL

Materials

PEG with a mass average of 3000 $gmol^{-1}$,tri-potassium citrate (anhydrous GR > 99% for analysis), sodium hydroxide (NaOH; mass purity > 0.99%), and sulfuric acid (95-97% H_2SO_4, GR > 95% for analysis) were calculated from Merck (Darmstadt, Germany) and no more purification was conducted when using PEG. The solution was prepared by distilled deionized water and all the other employed materials were analytically graded.

Apparatus and Procedure

Analytical Method. The calibration curve was determined by the analysis methods for salt and PEG concentrations. Moreover, the calibration plots for refractive indices and densities were prepared for the known polymer for the individual salt concentrations at 298K and the measured values were interpolated. According to this method, the average relative deviation of salt and polymer concentration was about 0.1% (wt). Therefore, the binary (PEG 3000 + water; sodium sulfate + water) and ternary (PEG 3000 + sodium sulfate + water) systems were prepared through addition (10 g) of the suitable mass for individual solution followed by the addition of double-distilled-deionized water in a 15 mL graduated tubes using an analytical balance (A&D., Japan, model GF300) with an accuracy of $\pm 10^{-4}$ g. Then, the Anton Paar oscillation U-tube densitometer (model: DMA 500) with a precision of $\pm 10^{-4}$ $g.cm^{-3}$ and a refractometer (CETI; Belgium) with a precision of 0.0001 nD were used to measure the densities and the refractive indices of each sample at 298 K, respectively. Moreover, the duplicate data measurement was employed and the average values of the parameters were reported.

The correlation of the physical properties in the ternary systems was obtained by a linear empirical expression.

The aim of the researchers was to decrease the mathematical complexity without losing accuracy.

$$Z = a + b \cdot w_p + c w_s + d w_p^2 + e w_s^2 + f w_p w_s \qquad (1)$$

Where Z may denote density or refractive index, w_p and w_s indicate the mass fractions of polymer and salt, respectively, and a, b and c are the fitting parameters. Then, the refractive index was plotted against polymer concentration to calibrate the different concentrations of salt.

Binodal Curve, TLL and STL. The binodal curve was obtained through the cloud-point method (also known as titration method).[21] The titration of the polymer and salt solutions of particular concentrations was conducted to make the solution turbid. The mass could determine the mixture composition So that after the formation of two phases and separate them, n_D and ρ measured and the amount of top and bottom phase salt and polymer in equation 1 was calculated. In this study, for preparation of aqueous two phase system, amounts PEG 3000+ potasiuum citrate + water were mixed in 15 mL graduated cylinder at 298.15 K to prepare 10 g of the feed samples based on the phase composition data attained from these experiments. Meanwhile, an appropriate ratio of lithium sulfate, sodium hydroxide and sulfuric acid was mixed, respectively, so that the pH values of the salt solutions could be accurately adjusted via a pH meter (827 pH, Lab, Metrohm, Swiss made). The contents of the test tubes were scrupulously put in vortexes for 5 min prior to their placement in the thermostatic bath of 298.15 K for 2 h. Later, the tubes were centrifuged (Hermle Z206A, Germany) at 6000 rpm for 5 min, therefore the top and bottom samples could be density, viscosity, and refractive indices of both top and bottom phases were measured at 298.15 K. An Anton Paar viscometer Lovis 2000 M with different capillary sizes (1.59 and 1.8 mm) for measuring range of 0.5–300 (mPa.s) with an accuracy of up to 0.5% was used to measure the viscosities of the solutions at 298.15 K.

Moreover, it can be recognized from the data shown in *Table* 1 that an increment in salt composition at a constant pH improved the PEG concentration in the top phase. The salt hydration impact can clarify this point.

The Tie-Line Length (TLL) for the different compositions of the two phases can be obtained by the equivalent

equation:

$$\mathrm{TLL} = \sqrt{(C_p^{top} - C_p^{bottom})^2 + (C_s^{bottom} - C_s^{top})^2} \quad (2)$$

The Slope of the Tie-Line (STL) is given by the ratio of the difference between the polymer (C_P) and salt (C_S) concentrations in the top and bottom phases as presented in Eq. 3:

$$\mathrm{STL} = \frac{c_p^{top} - c_p^{bottom}}{c_s^{bottom} - c_s^{top}} \quad (3)$$

The equilibrium phase compositions, tie line data and physical properties of the top and bottom phases are shown in *Tables* 8. Experiments were carried out with three feed solutions containing PEG 3000+tri-potassium citrate + water at three pH values. The experimental results for the feed solutions and additionally for the resulting coexisting phases are also given in *Table* 1.

Binodal Curve and TLL Correlation. For the binodal data correlation, the Merchuk equation[30] is a proper tool to reproduce the binodal curves of the investigated systems.

$$w_p = ae^{(bw_s^{0.5} - cw_s^3)} \quad (4)$$

Where a, b and c represent the fitting parameters and w_p and w_s demonstrate the polymer and salt mass fractions, respectively. The binodal data of the above expression were correlated by least-squares regression.

The reliability of the measured tie-line compositions was checked by Othmer-Tobias (Eq. 5) and Bancroft (Eq. 6) correlation equations.

***Table* 2.** Values of parameters of equation 3 for PEG 3000 + potassium citrate + water at different pH values

pH	*a*	*b*	*c*	R^2
8.33	10.8239	-1.4721	0.1421	0.9998
9.60	8.0751	-1.0574	0.2278	0.9998
10.52	7.8533	-1.1095	0.1892	0.9997

$$\left(\frac{1-w_{pt}}{w_{pt}}\right) = k\left(\frac{1-w_{sb}}{w_{sb}}\right)^n \quad (5)$$

$$\left(\frac{w_{wb}}{w_{sb}}\right) = k_1\left(\frac{w_{wt}}{w_{pt}}\right)^r \quad (6)$$

Where w_{pt} is the mass fraction of PEG 3000 in the top phase, w_{sb} is the mass fraction of Li_2So_4 in the bottom phase, w_{wb} and w_{wt} are the mass fractions of water in the bottom and top phases, respectively, and k, n, k_1, and r are the parameters. The values of the parameters are given in *Table* 3.

THERMODYNAMIC FRAMEWORK

In this study, the extended UNIQUAC,[22] UNIFAC,[23] modified UNIQUA-FV[24] and Virial-(Mobalegholeslam & Bakhshi)[25] were used to calculate the phase equilibria of $K_3C_6H_5O_7$ + PEG 3000 + H_2O (pH = 8.33, 9.60 and 10.52) systems. The excess Gibbs energy, G^E, was expressed as the sum of three contributions:

$$G^E = G^{LR} + G^{SR} + G^{com} \quad (7)$$

In equation (1), G^{LR} is the long-range interaction contribution, which stands for the electrostatic interactions between

***Table* 1.** Phase composition, tie-line data and physical properties of PEG 3000+ potassium citrate + water aqueous two-phase system at 298.15 K and 0.1 MPa

pH	Total system (%mass)		Top phase					Bottom phase					TLL	-STL
	$100\,w_p$	$100\,w_s$	$100\,w_p$	$100\,w_s$	$\rho(\pm0.0001)$ $kg\cdot m^{-3}$	n_D (±0.0001)	$\eta(\pm0.01)$ $mPa\cdot s$	$100\,w_p$	$100\,w_s$	$\rho(\pm0.0001)$ $kg\cdot m^{-3}$	n_D (±0.0001)	$\eta(\pm0.001)$ $mPa\cdot s$		
8.33	21.00	13.00	32.25	6.56	1.0931	1.3883	17.98	1.89	23.82	1.1589	1.3686	1.999	34.92	1.76
	20.00	13.00	30.89	6.89	1.0926	1.3868	16.55	1.99	23.19	1.1576	1.3679	2.122	33.18	1.77
	19.00	13.00	29.12	7.51	1.0905	1.3851	14.65	2.12	22.69	1.1522	1.3674	2.445	30.97	1.78
	18.00	13.00	27.61	7.94	1.0881	1.3836	11.74	2.30	22.10	1.1430	1.3668	2.885	29.00	1.79
9.60	21.00	13.00	33.84	6.12	1.0951	1.3900	17.75	1.21	24.07	1.1609	1.3680	1.320	37.24	1.82
	20.00	13.00	31.99	6.57	1.0944	1.3880	14.11	1.93	23.00	1.1561	1.3675	1.480	34.25	1.83
	19.00	13.00	31.01	6.81	1.0942	1.3869	10.75	2.18	22.48	1.1516	1.3672	1.693	32.81	1.84
	18.00	13.00	30.00	7.05	1.0940	1.3858	7.178	2.49	21.89	1.1472	1.3668	1.727	31.25	1.85
10.52	21.00	13.00	35.63	5.19	1.0945	1.3913	17.03	2.00	22.88	1.1632	1.3675	1.710	38.33	1.85
	20.00	13.00	34.44	5.49	1.0944	1.3900	16.28	1.88	23.34	1.1543	1.3679	1.767	36.80	1.86
	19.00	13.00	33.29	5.73	1.0928	1.3887	12.93	2.13	22.39	1.1493	1.3670	1.810	35.33	1.87
	18.00	13.00	32.11	6.12	1.0898	1.3875	7.397	2.40	21.89	1.1449	1.3667	1.888	33.63	1.88

Standard uncertainties: $u(wi) = 0.002$; $u(P) = 5$ kPa; $u(T) = 0.05$ K.

***Table* 3.** Values of the parameters of *Eqs.* 1 and 2 for PEG3000 + Lithium sulfate + water at different pH values

pH	k	n	R^2	k_1	r	R^2
8.33	0.00245	4.154	0.9999	5.7839	0.2722	0.9998
9.60	0.00140	4.555	1.0000	5.6192	0.2812	0.9924
10.52	0.01281	3.050	1.0000	4.6495	0.3875	0.9967

the ions. G^{SR} represents the short-range interaction contribution that reflects the non-electrostatic interactions between every part of the solution. G^{com} denotes the combinatorial contribution and specifies the configuration entropy of the system's constituent particles. Subsequently, the activity coefficient of the component, *i*, is given as the sum of three contributions:

$$\ln\gamma_i = \ln\gamma_i^{LR} + \ln\gamma_i^{SR} + \ln\gamma_i^{com} \tag{8}$$

Long-Range Interaction Contribution

The long range coefficient of non-ionic components such as water polymer is calculated as below:

$$\ln\gamma_i^{LR} = \frac{2AV_i d}{b^3}[1+bI^{0.5} - (1+bI^{0.5})^{-1} - 2\ln(1+bI^{0.5})] \tag{9}$$

The other way of writing the mean ionic activity coefficient of electrolyte *i* is:

$$\ln\gamma_{\pm}^{LR} = \frac{|Z_a Z_c| AI^{0.5}}{1+bI^{0.5}} \tag{10}$$

Where I is ionic strength and V_i is the molar volume of the non-ionic component. Also, if the distances between the ions are less than 4A°, A and b are obtained by:

$$A = 1.32775\times10^5\left(\frac{d^{0.5}}{(DT)^{1.5}}\right) \tag{11}$$

$$b = 6.359696\times\frac{d^{0.5}}{(DT)^{0.5}} \tag{12}$$

D and d are the dielectric constant and the density of the mixture respectively. The resulting solution is considered as the combination of a solvent and a pseudo-solvent polymer and obtained by:

$$D = \sum\Phi_k^{'}D_k \tag{13}$$

$$d = \sum\Phi_k^{'}d_k \tag{14}$$

Where $\Phi_k^{'}$ is volume fraction of the non-ionic component and it is calculated by:

$$\Phi_k^{'} = \frac{n_k V_k}{\sum_{i\neq ion} n_i V_i} \tag{15}$$

The Extended UNIQUAC Model

The reason for employing the extended UNIQUAC equation was the calculation of the short range interaction contribution of activity coefficient (Eq. 11):

$$\ln\gamma_i = \ln\left(\frac{\phi_i}{x_i}\right) + \frac{Z}{2}q_i\ln\frac{\theta_i}{\phi_i} + l_i - \frac{\phi_i}{x_i}\sum_{j=1}^{m}x_j l_j + q_i\left[1 - \ln\left(\sum_{j=1}^{m}\theta_j\tau_{ji}\right) - \sum_{j=1}^{m}\frac{\theta_j\tau_{ij}}{\sum_{k=1}^{m}\theta_k\tau_{kj}}\right] \tag{16}$$

$$l_i = \frac{Z}{2}(r_i - q_i) - (r_i - 1) \tag{17}$$

Subscripts i and j show the components of the systems. x_i, is mole fraction of component i, and can be calculated by the following equations in an electrolyte solution:

$$x_w = \frac{n_w}{v_s n_s + n_p + n_{w\,Gu}} \tag{18}$$

$$x_p = \frac{n_p}{v_s n_s + n_p + n_w} \tag{19}$$

$$x_s = \frac{v_s n_s}{v_s n_s + n_p + n_w} \tag{20}$$

Where, v_s is the stoichiometric coefficient of zinc sulfate salt. n_i is the number of moles of component i in each aqueous phase. Z shows the coordination number and set equal to 10. Subscripts *w, p, s* show the water, polymer and zinc sulfate, respectively. Volume fraction ϕ_i and a surface fraction θ_i of each component are calculated by the following equations:

$$\phi_i = \frac{x_i r_i}{\sum_i x_i r_i} \tag{21}$$

$$\theta_i = \frac{x_i q_i}{\sum_i x_i q_i} \tag{22}$$

Where, r and q are volumetric and surface parameters of van der Waals, respectively. Also, τ_{ij} is Boltzmann factor and defined as:

$$\tau_{ij} = \exp\left(\frac{-a_{ij}}{T}\right) \tag{23}$$

Where, T is temperature and. u_{ij} and u_{jj} are interaction energy parameters of similar and non-similar components, respectively. It is obvious that $\tau_{ii} = \tau_{jj} = 1$.

The modified UNIQUA-FV Model

In the modified UNIQUA-FV model, the activity coefficient of component i is obtained by:[24]

$$\ln\gamma_i^{M\,UNIQUAC-FV} = \ln\gamma_i^{Com+FV} + \ln\gamma_i^{SR} \tag{24}$$

In equation (18), the first part stands for the combinatorial and the second one for the short range part. In this research modified Freed-FV model was employed to obtain the combinatorial activity coefficient. The activity coefficients of the components were calculated according to the following equation:

$$\ln\gamma_i^{Com+FV} = \ln\frac{\phi_i}{x_i} + \frac{z}{2}q_i\ln\frac{\theta_i}{\phi_i} + l_i - \frac{\phi_i}{x_i}\sum_j x_j l_j + \ln\left(\frac{\phi_i^{FV}}{\phi_i^h}\right) + \left(\frac{\phi_i^h - \phi_i^{FV}}{x_i}\right) + 0.2\left(\frac{\phi_i^{FV}}{x_i}\right)^2 - 0.2\left(\frac{\phi_i^h}{x_i}\right)^2 \tag{25}$$

Where ϕ_i^h denotes the fraction of hardcore volume associated with component i:

$$\phi_i^h = \frac{x_i v_i^h}{\sum_j x_j v_j^h} \tag{26}$$

Where ϕ_i^{FV} denotes the fraction of free volume associated with component i:

$$\phi_i^{FV} = \frac{x_i(v_i - v_i^h)}{\sum_j x_j(v_j - v_j^h)} \tag{27}$$

Where x_i represents the mole fraction of component i, v_i dentoes molar volume of component I, and v_i^h is the molar hardcore volume of component i.

The short range ($\ln\gamma_i^{SR}$) part of the activity coefficient is defined as:

$$\frac{1}{q_w}\ln\gamma_w^{SR} = 1 - \ln\left(\frac{\theta_p H_{p,w} + (\theta_c+\theta_a)H_{ca,w} + \theta_w}{\theta_w+\theta_c+\theta_a+\theta_p}\right) - \left(\frac{\theta_w((\theta_a+\theta_c)(1-H_{ca,w}) + \theta_p(1-H_{p,w}))}{(\theta_w+\theta_c H_{ca,w}+\theta_a H_{ca,w}+\theta_p H_{p,w})(\theta_w+\theta_c+\theta_a+\theta_p)}\right) - \left(\frac{\theta_c(\theta_a(H_{w,ca}-1)+\theta_p(H_{w,ca}-H_{p,ca}))}{(\theta_w H_{w,ca}+\theta_a+\theta_p H_{p,ca})(\theta_w+\theta_a+\theta_p)}\right) - \left(\frac{\theta_a(\theta_c(H_{w,ca}-1)+\theta_p(H_{w,ca}-H_{p,ca}))}{(\theta_w H_{w,ca}+\theta_c+\theta_p H_{p,ca})(\theta_w+\theta_c+\theta_p)}\right) - \left(\frac{\theta_p(\theta_p(H_{w,p}-1)+(\theta_a+\theta_c)(H_{w,p}-H_{ca,p}))}{(\theta_p+(\theta_c+\theta_a)H_{ca,p}+\theta_w H_{w,p})(\theta_w+\theta_c+\theta_a+\theta_p)}\right) \tag{28}$$

$$\frac{1}{q_p}\ln\gamma_p^{SR} = \ln H_{w,p} + H_{p,w} - \ln\left(\frac{\theta_w H_{w,p}+\theta_c H_{ca,p}+\theta_a H_{ca,p}+\theta_p}{\theta_w+\theta_c+\theta_a+\theta_p}\right) - \left(\frac{\theta_w((\theta_a+\theta_c)(H_{p,w}-H_{ca,w})+\theta_w(H_{p,w}-1))}{(\theta_w+\theta_c H_{ca,w}+\theta_a H_{ca,w}+\theta_p H_{p,w})(\theta_w+\theta_c+\theta_a+\theta_p)}\right) - \left(\frac{\theta_c(\theta_a(H_{p,ca}-1)+\theta_w(H_{p,ca}-H_{w,ca}))}{(\theta_a+\theta_p H_{p,ca}+\theta_w H_{w,ca})(\theta_w+\theta_a+\theta_p)}\right) - \left(\frac{\theta_a(\theta_c(H_{p,ca}-1)+\theta_w(H_{p,ca}-H_{w,ca}))}{(\theta_c+\theta_p H_{p,ca}+\theta_w H_{w,ca})(\theta_w+\theta_a+\theta_p)}\right) - \left(\frac{\theta_p((\theta_a+\theta_c)(1-H_{ca,p})+\theta_w(1-H_{w,p}))}{(\theta_w H_{w,p}+\theta_c H_{ca,p}+\theta_a H_{ca,p}+\theta_p)(\theta_w+\theta_c+\theta_a+\theta_p)}\right) \tag{29}$$

$$\frac{1}{Z_c q_p}\ln\gamma_c^{SR} = \ln H_{w,c} + H_{c,w} - \ln\left(\frac{\theta_p H_{p,ca}+\theta_a+\theta_w H_{w,ca}}{\theta_w+\theta_a+\theta_p}\right) - \left(\frac{\theta_w(\theta_p(H_{ca,w}-H_{p,w})+\theta_w(H_{ca,w}-1))}{(\theta_w+\theta_c H_{ca,w}+\theta_a H_{ca,w}+\theta_p H_{p,w})(\theta_w+\theta_c+\theta_a+\theta_p)}\right) - \left(\frac{\theta_a(\theta_p(1-H_{p,ca})+\theta_w(1-H_{w,ca}))}{(\theta_w H_{w,ca}+\theta_c+\theta_p H_{p,ca})(\theta_w+\theta_c+\theta_p)}\right) - \left(\frac{\theta_p(\theta_p(H_{ca,p}-1)+\theta_w(H_{p,ca}-H_{w,p}))}{(\theta_p+\theta_w H_{w,p}+\theta_a H_{ca,p}+\theta_c H_{ca,p})(\theta_w+\theta_c+\theta_a+\theta_p)}\right) \tag{30}$$

This equation can be expressed in the same forms as activity coefficient of the cation (c) by replacing the subscript of c with that of a and a with c.

The mean ionic activity coefficient of an electrolyte ($K_3C_6H_5O_7$) with cation and anion can be obtained using Equation 31:

$$\ln\gamma_{\pm K_3C_6H_5O_7} = \frac{v_c\ln\gamma_c + v_a\ln\gamma_a}{v_c+v_a} \tag{31}$$

The UNIFAC Model

The functional groups that form the structures of the compounds are explained by the UNIFAC model in which each functional group provides a distinctive contribution to the compound property. Moreover, the interaction parameters are applicable to the systems with several components as they are obtained by taking the thermodynamically consistent data for an account for a small number of groups.[23] The activity coefficient in the UNIFAC model is provided by a combinatorial part (γ_i^C) for entropy effects derived from the differences in molecular size and shape,

and a residual part (γ_i^R) for energetic interactions between the functional groups in the mixture.

$$\ln\gamma_i^{UNIFAC} = \ln\gamma_i^C + \ln\gamma_i^R \tag{32}$$

The UNIFAC model the combinatorial part is given by:

$$\ln\gamma_i^C = 1-\phi_i + \ln\phi_i - \frac{Z}{2}q_i\left(1-\frac{\phi_i}{F_i}+\ln\left(\frac{\phi_i}{F_i}\right)\right) \tag{33}$$

$$\phi_i = \frac{r_i}{\sum_j r_j x_j} \quad \& \quad F_i = \frac{q_i}{\sum_j r_i x_j} \tag{34}$$

$$r_i = \sum v_k^{(i)} R_k \quad \& \quad q_i = \sum v_k^{(i)} Q_k \tag{35}$$

Where x_i is the mole fraction of component i in the liquid phase and $v_k^{(i)}$ is the number of groups of type k in component i. R_k denotes van der Waals group volume and Q_k shows the surface, for group k, and Z is the coordination number a value between 4 and 12 depending on the type of packing as defined in lattice theory. Furthermore, for typical liquids z value is 10. The residual part of the activity coefficient is obtained from the following equations:

$$\ln\gamma_i^R = \sum v_k^{(i)}(\ln\Gamma_K - \ln\Gamma_k^{(i)}) \tag{36}$$

$$\ln\Gamma_k = Q_K\left(1-\ln\left(\sum_m \theta_m\psi_{mk}\right) - \sum_m \frac{\theta_m\psi_{km}}{\sum_n \theta_m\psi_{nm}}\right) \tag{37}$$

Where the group area fraction, θ_m, and group mole fraction, X_m, are given by the equations:

$$\theta_m = \frac{Q_m X_m}{\sum_n Q_n X_n} \tag{38}$$

$$X_m = \frac{\sum_j V_m^{(i)} X_j}{\sum_j \sum_n V_n^{(i)} X_j} \tag{39}$$

The parameter ψ_{mn} contains the group interaction parameter, a_{nm} according to the equation:

$$\psi_{nm} = \exp\left(\frac{-a_{nm}}{T}\right) \tag{40}$$

Virial-(Mobalegholeslam & Bakhshi) model

In the Virial-(Mobalegholeslam & Bakhshi) model, the activity coefficient of component i is obtained as [25]:

$$\ln\gamma_i^{Virial-(M\&B)} = \ln\gamma_i^{Com} + \ln\gamma_i^{SR} \tag{41}$$

In equation (22), the first part stands for the combinatorial and the second one for the short range part. Moreover, the short-range ($\ln\gamma_i^{SR}$) part of the activity coefficient is defined as:

$$\ln\gamma_w = -0.5[B_{pp}(0.5(r_p-1)m_p)^2 + B_{ss}m_s^2 + B_{sp}m_p m_s(0.5(r_p-1))] \tag{42}$$

$$\ln\gamma_p = \frac{1000}{Mw}[0.5(r_p-1)m_p(B_{pp}0.5(r_p-1)m_p) + B_{ps}m_s] \tag{43}$$

$$\ln\gamma_s = \frac{1000}{Mw}m_s[B_{ss}m_s + B_{ps}0.5(r_p-1)m_p] \tag{44}$$

The subscripts w, p, and s stand for the water, polymer and salt, respectively. The second virial coefficient B_{ij} is provided in the Equation 40:

$$B_{ij} = B_{ij}^{(0)} + B_{ij}^{(1)} \times \frac{2}{\alpha^2 I}[1-(1+\alpha(I)^{0.5})\exp(-\alpha(I)^{0.5})] \tag{45}$$

Where I is ionic strength and α is set equal to 2 $Kg^{1/2}/mol^{1/2}$. Osmotic virial coefficients have been related to temperature as:

$$B_{ij}^{(0)} = B_{ij}^{\alpha(0)} + \frac{B_{ij}^{\beta(0)}}{T} \tag{46}$$

$$B_{ij}^{(1)} = B_{ij}^{\alpha(1)} + \frac{B_{ij}^{\beta(1)}}{T} \tag{47}$$

The combinatorial part ($\ln\gamma_i^{Com}$) of the activity coefficient is defined as:

$$Ln\gamma_i^{Com} = Ln\left(\frac{\phi_i^{FV}}{x_i}\right) + 1 - \left(\frac{\phi_i^{FV}}{x_i}\right) + f_i^{Freed-FV} \tag{48}$$

The last term of Eq. 29 suggested as follows:

$$f_i^{Freed-FV} = R_i^{FV}\left[\sum_j \beta_{ji}^{FV}\phi_j^{FV}(1-\phi_j^{FV}) - 0.5\sum_{j\neq i}\sum_{k\neq i}\beta_{jk}^{FV}\phi_j^{FV}\phi_k^{FV}\right] \tag{49}$$

$$\beta_{ji}^{FV} = \alpha_{ij}\left(\frac{1}{R_j^{FV}} - \frac{1}{R_i^{FV}}\right) \tag{50}$$

In the above equations, x_i denotes mole fraction of component i and α_{ij} indicates the set equal to 0.2. Also, R_j^{FV} is calculated as the ratio of v_j^{FV} to v_i^{FV}, v_i^{FV} and is the molar volume of the solvent (water).

RESULTS AND DISCUSSION

Analytical Method

Table 4 contains the fitting parameters for calibration

***Table* 4.** Refractive index and density calibration constants for a binary system

z	*a*	*b*	*c*	*d*	*e*	*f*
n_D	1.3328	0.01141	0.0132	0.0001	0.0002	1.0000
ρ/g.cm^3	0.9972	0.0601	0.0157	0.0003	0.0028	1.0000

curves. The provided empirical equation was in agreement with the experimental binodal data with high accuracy.

Binodal Data

The binodal data obtained from the turbidimetric titrations of PEG 3000+ tri-potassium citrate + water mixtures at 298.15 K at different pH values (8.33, 9.60, and 10.52) are presented in *Table* 5.

Effect of pH on Binodal Curves

The experimental and correlated binodal curves of the study systems are shown in *Fig.* 1.

***Table* 5.** Binodal curve data of the PEG 3000+ potassium citrate + water system at 298.15 K and 0.1 MPa at different pH values

pH = 8.33		pH = 9.60		pH = 10.52	
100 w_p	100 w_s	100 w_p	100 w_s	100 w_p	100 w_s
47.34	3.10	46.06	2.79	48.27	1.92
39.89	4.48	43.58	3.25	43.29	2.83
37.18	5.20	40.85	4.01	33.51	5.52
30.87	6.76	35.56	5.45	30.61	6.39
29.74	7.02	30.04	7.31	23.14	9.23
25.65	8.32	18.52	11.42	19.09	10.94
19.34	11.06	9.89	15.06	15.69	12.72
11.45	14.69	5.59	17.89	15.41	12.64
8.07	16.92			8.62	16.15
6.21	18.26			5.93	17.76
4.74	19.65				
4.59	19.75				
1.79	23.22				

Standard uncertainties: $u(wi) = 0.002$; $u(P) = 5$ kPa; $u(T) = 0.05$ K.

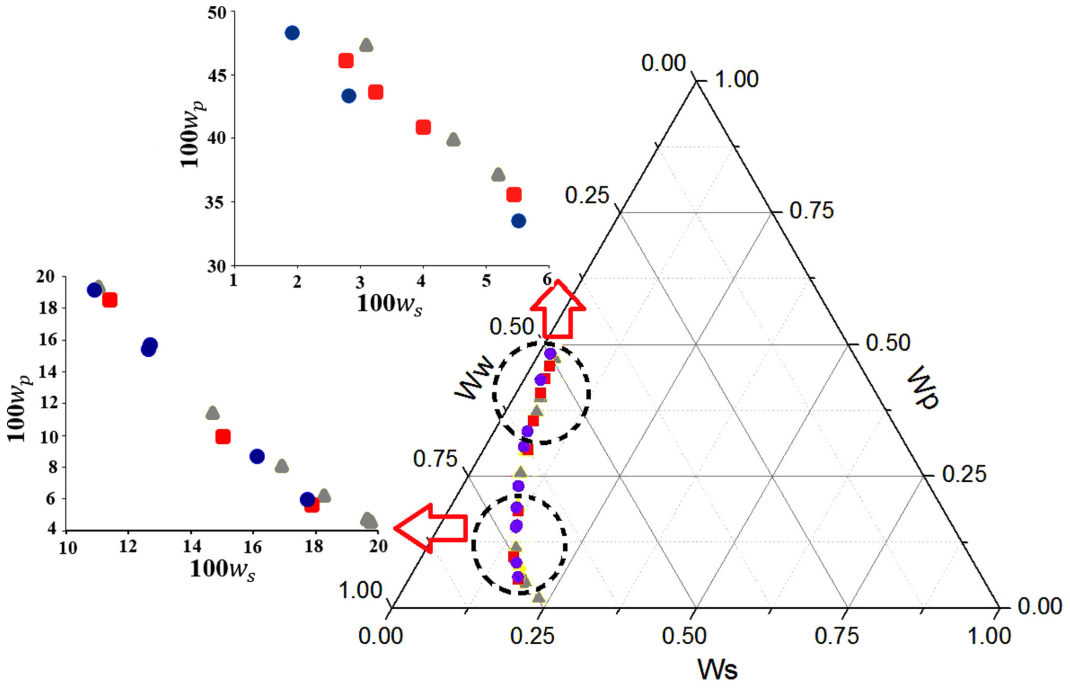

***Figure* 1.** The experimental and correlated binodal curves of PEG 3000+ potassium citrate + water ATPSs at pH=10.52: (●), pH=9.60: (■), pH=8.33: (▲).

Also, the effect of pH on the phase-forming ability of biphasic systems containing PEG 3000+ potassium citrate system is illustrated in *Figs* 3. Accordingly, the figure indicated that the two-phase area was expanded and the binodal curve changed into downward manner following the increase in pH of the medium. This suggests that the formation of ATPSs asks for the smaller concentration of the phase polymers. Furthermore, the findings of the other studies confirmed this the change of the mixture into a two-phase system after taking a sample with a known composition on the binodal curve and increasing its pH.[32,33]

The effect of pH on the binodal location can be explained in two ways: changing the charge of the solute and altering the ratio of the charged species present.[33] Accordingly, it was found that hydrogen-bond interactions of PEG are weakened at higher pH. Moreover, studies suggested that salting-out phenomenon is responsible for the depression of the cloud point after increasing pH as a consequence of weakening of the PEG−solvent interaction.[33]

This behavior can be explained based on the salt's ability to promote the water structure. According to the water structure-promoting capability (known as kosmotropicity) of salts, when a kosmotropic salt like sodium citrate, potassium phosphate, or magnesium sulfate is dissolved in an aqueous solution, the ionic hydration process will occur, and salt ions will be surrounded by a layer of water molecules.[32] Moreover, the reason for the water molecules structuring and immobilization are to reduce their function, as a solvent to other molecules.[32] In this case, when a kosmotropic salt is added to an aqueous solution of a hydrophilic PEG, they compete with each other for the water molecules. The hydration and the solubility of PEG would decrease due to the stronger affinity of salt ions for the water relative to PEG, therefore, the hydrophilic PEG was salted-out and excluded from the rest of the solution as a separate phase at certain concentrations.[32]

The equilibrium phase compositions, tie-line data and physical properties of the top and bottom phases are shown in *Table* 8. The experiments were carried out with three feed solutions containing PEG 3000+ tri-potassium citrate + water at all three pH values.

In *Fig*. 2,3 and 4, the effects of pH on the equilibrium phase compositions and the slope and length of the tie lines have been represented for the PEG3000 + tri-potassium citrate + H_2O system. An increase in pH would result in TLL and STL augmentations in the above system, which was possibly caused due to the reduction in the solution hydrodynamic volume. Similarly, a comparable conduct

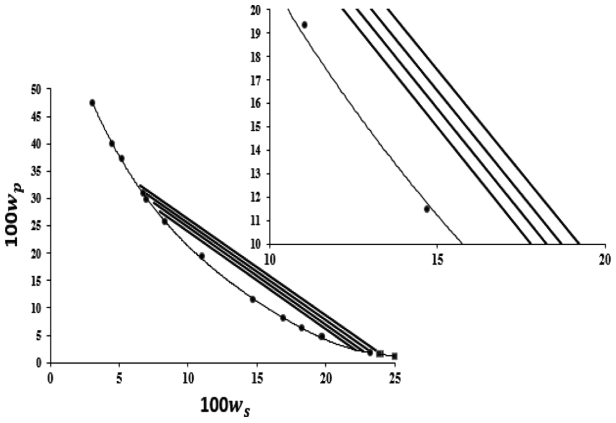

***Figure* 2.** Tie lines for PEG 3000 + potassium citrate + water at pH=8.33 ●, experimental; ■, calculated from eqs 36, —, calculated from eqs 39 and 40.

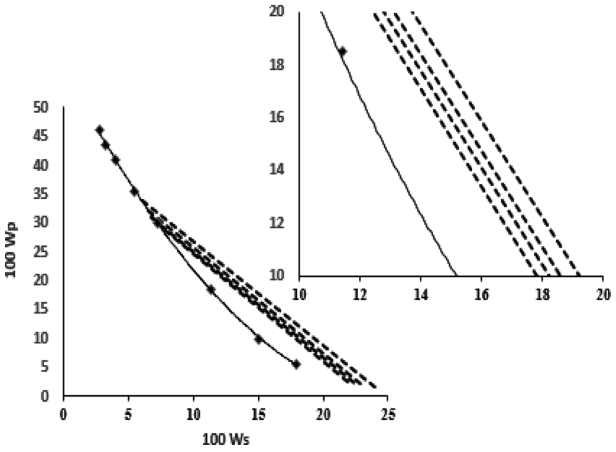

***Figure* 3.** Tie lines for PEG 3000 + potassium citrate + water at pH=9.60 ■, experimental; ▲calculated from eqs 36; ---, calculated from eqs 39 and 40.

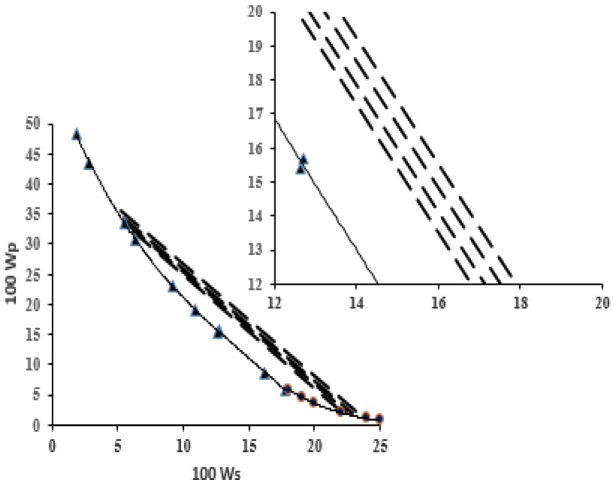

***Figure* 4.** Tie lines for PEG 3000 + potassium citrate + water at pH=10.52▲, experimental; ●, calculated from eqs 35; - - -, calculated from eqs 39 and 40.

has been portrayed in article.[7] Moreover, the studies reported that the slope and the length of the equilibrium tie-lines for the PEG3000 + tri-potassium citrate ATPS increased by pH increment and there was a direct relationship between the increase in pH and the volume of salt-rich phase at the expense varying pH.[7,31,34]

Moreover, the current study considered the TLL effects on some other variables such as the densities, dynamic viscosities, and kinematic viscosities of the aqueous two-phase systems. Accordingly, the density (Δρ) and viscosity (Δη) differences between the phases were found to increase and decrease with TLL and pH enhancements, respectively. Besides, a linear relationship was discovered between the density and viscosity differences between the phases and TLL as shown in *Figs* 5, 6, and 7. Similarly, some comparable conducts were represented in.[32,33].

Thermodynamic Modeling

The extended UNIQUAC,[22] UNIFAC,[23] modified UNIQUAC-FV[24] and Virial-(Mobalegholeslam & Bakhshi)[25] and models connected the experimental data by minimizing the objective function presented below:

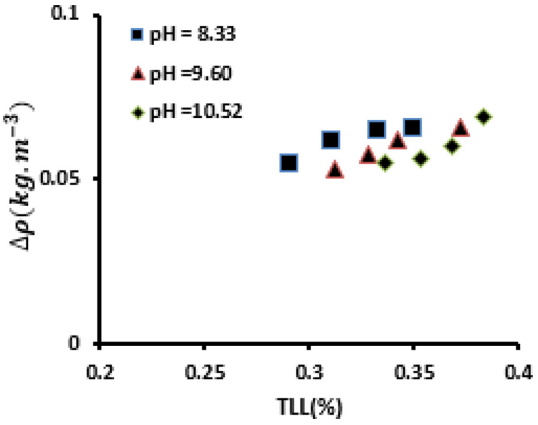

***Figure* 5.** The relationship between density difference (Δρ) and Tie-Line Length (TLL) for the PEG 3000 +tri potassium citrate + water system at different pH values.

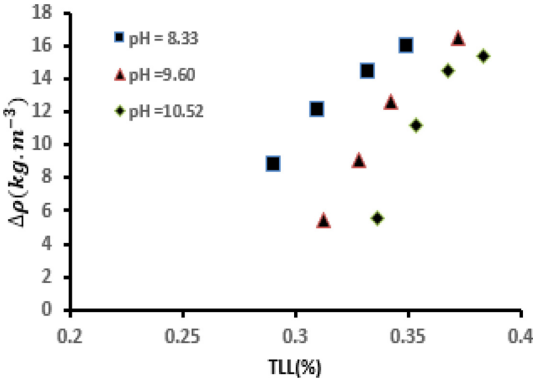

***Figure* 6.** The relationship between viscosity difference (Δη) and Tie-Line Length (TLL) for the PEG 3000 +tri potassium citrate + water system at different pH values.

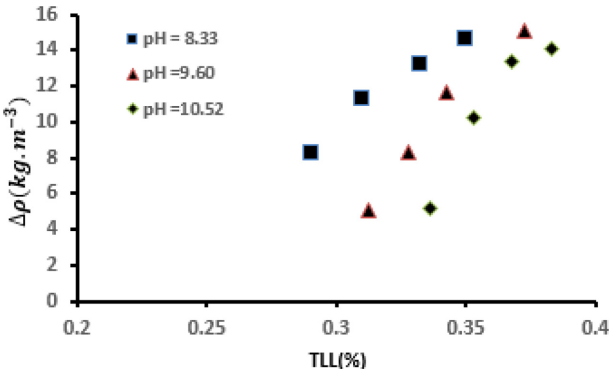

***Figure* 7.** The relationship between kinematic viscosity difference (Δν) and Tie-Line Length (TLL) for the PEG 3000 +tri potassium citrate + water system at different pH values.

$$OF = \sum_p \sum_l \sum_j (w_{p,lj}^{cal} - w_{p,lj}^{exp})^2 \quad (51)$$

where $w_{p,lj}$ denotes the weight fraction of the j species in the phase p for l-th tie-line. In equation (43), the species j can be a polymer, salt, or solvent molecule and *cal* indicates the calculated values, whereas the experimental values are shown with *exp* superscript. The equilibrium condition was used to correlate the liquid-liquid equilibrium records.

$$(x_i\gamma_i)^{top} = (x_i\gamma_i)^{bottom} \quad (52)$$

Apparently, the ideal value for the sum of mole fractions of the three components in every phase is the equivalence to unity, then the mass balance equation would be an appropriate tool ascertain the calculated values. Mole fraction calculated values are derived from the stated equations and a suitable model of activity coefficient.

In the current research whenever was possible, the authors used the available binary experimental data reported in the literature to fit the binary parameters of mentioned models. The binary interaction parameters of extended UNIQUAC, Virial-(Mobalegholeslam & Bakhshi) and modified UNIQUAC-FV model for the water-polymer system have been calculated by minimizing the difference between the experimental vapor-liquid equilibrium data reported by Ninn et al.[26] and the calculated values obtained by the mentioned model. Also, binary interaction parameters of water + salt binary system have been calculated in the same procedure using related VLE experimental data in the reference.[27] In this study, the interaction parameters of the salt and poly-

mer for the extended UNIQUAC, Virial-(Mobalegholeslam & Bakhshi) and modified UNIQUAC-FV models were obtained from the experimental data of the LLE. The comparison of the interaction parameters of the VLE data indicated a quite successful agreement with the LLE system in all of these models. The fitting parameters of the extended UNIQUAC, Virial-(Mobalegholeslam & Bakhshi) and modified UNIQUAC-FV models, together with the respective deviations, are summarized in *Table* 6. Moreover, interaction parameters of UNIFAC model were calculated on the basis of the interaction parameters of LR de Lemos et al.,[28] and VM De Andrade et al..[29] The obtained interaction parameters were listed in *Table* 7. Moreover, *Table* 8 shows the deviation of experimental data with three different models of modified UNIQUAC-FV, extended UNIQUAC, Virial-(Mobalegholeslam & Bakhshi) and UNIFAC models. *Fig.* 8, 9, and 10 shows the composition of the salt, polymer, and water obtained by the extended UNIQUAC, modified UNIQUAC-FV, Virial-(Mobalegholeslam & Bakhshi) and UNIFAC models besides the experimental values. However, the Virial-(Mobalegholeslam & Bakhshi) model is superior to the other three models.

CONCLUSION

The new experimental results were presented for the LLE data of the PEG 3000 + tri-potassium citrate+ water system at various pH values of 8.33, 9.60 and 10.52 at 298.15 K. It was found that the two-phase area was expanded with increasing pH. Moreover, the pH enhancement resulted in a decrease in the slope of the equilibrium tie-lines; however, the length of tie-lines increased for the investigated biphasic system. The calibration method was applied to measure both the refractive index and density of the phases. The

***Table* 6.** The values of the parameters of the extended UNIQUAC, modified UNIQUAC-FV and Virial-(Mobalegholeslam & Bakhshi) model for the PEG 3000 (*p*) + tri-potassium citrate (*ca*) + water (*w*) system at pH = (8.33, 9.60, and 10.52)

Systems			extended UNIQUAC model						
	a^a_{wp}	a^a_{pw}	AAD%[b]	a_{wca}	a_{caw}	AAD%	a_{pca}	a_{cap}	SD%[c]
pH(8.33)	177.5398	-77.5106	0.0856	10418.47	1637.6	0.0036	1768.5	5751.98	16.37×10^{-2}
pH(9.60)									17.91×10^{-2}
pH(10.52)									17.89×10^{-2}
			modified UNIQUAC-FV model						
	u_{wp}	u_{pw}	AAD%	u_{wca}	u_{caw}	AAD%	u_{pca}	u_{cap}	SD%
pH(8.33)	-201.58	-63.20	0.0311	-1905.8	117.5	0.0018	573.80	-1191.07	4.02×10^{-2}
pH(9.60)									4.55×10^{-2}
pH(10.52)									4.12×10^{-2}

			Virial-(Mobalegholeslam & Bakhshi) model										
	$10^3\times B^{\alpha(0)d}_{PP}$	$10^3\times B^{\beta(0)d}_{PP}$	AAD%	$10^3\times B^{\alpha(0)}_{SS}$	$10^3\times B^{\beta(0)}_{SS}$	$10^3\times B^{\alpha(1)}_{SS}$	$10^3\times B^{\beta(1)}_{SS}$	AAD%	$B^{\alpha(0)}_{PS}$	$B^{\beta(0)}_{PS}$	$B^{\alpha(1)}_{PS}$	$B^{\beta(1)}_{PS}$	SD%
pH(8.33)	54.0093	9.4100	0.081	0.207	0.005	-0.15	-2.35	1.21×10^{-5}	5.027	-1.195	-0.280	-9.470	3.35×10^{-2}
pH(9.60)													3.98×10^{-2}
pH(10.52)													3.89×10^{-2}

[a]Calculated and reported by Pirdashti et al. [21]

[b]$AAD\% = \frac{100}{NP}\sum_{n-1}^{NP}\left|\frac{a^{cal}_{wn}-a^{exp}_{wn}}{a^{exp}_{wn}}\right|$ where N_P is the number of experimental data points.

[c]$SD\% = 100\left(\frac{OF}{6N}\right)$; where N is the number of tie-lines.

[d]Calculated and reported by Mobalegholeslam and Bakhshi. [25]

***Table* 7.** Group interaction parameters (a_{nm}) of our UNIFAC model.[27,28]

	CH_2	CH_2CH_2O	OH	K^+	$(C_6H_5O_7)^{3-}$	H_2O
CH_2	0	1167.5	−1105.9	−25.584	−1300.4	−471.26
CH_2CH_2O	2298.0	0	91.546	1731.1	930.51	−0.91698
OH	6159.7	−285.50	0	−1164.5	−366.04	325.88
K^+	−151.22	214.33	2.5989	0	−1451.89[a]	−28.745
$(C_6H_5O_7)^{3-}$	285.67	−213.67	17.846	6811.04[a]	0	−279.00
H_2O	324.99	0.12082	16.431	−29.828	292.34	0

[a]Calculated by authors

***Table* 8.** The deviation (*SD %*) values of liquid–liquid equilibrium calculation for PEG 3000 + tri-potassium citrate + water systems with different pH using UNIFAC, Virial-(Mobalegholeslam & Bakhshi), extended UNIQUAC and modified UNIQUAC-FV models

Systems	UNIFAC	Virial-(Mobalegholeslam & Bakhshi)	extended UNIQUAC	modified UNIQUAC-FV
PEG 3000 + tri-potassium citrate + water system at pH 8.33	34.95×10^{-2}	3.35×10^{-2}	16.37×10^{-2}	4.02×10^{-2}
PEG 3000 + tri-potassium citrate + water system at pH 9.60	21.85×10^{-2}	3.98×10^{-2}	17.91×10^{-2}	4.55×10^{-2}
PEG 3000 + tri-potassium citrate + water system at pH 10.52	19.09×10^{-2}	3.89×10^{-2}	17.15×10^{-2}	4.12×10^{-2}

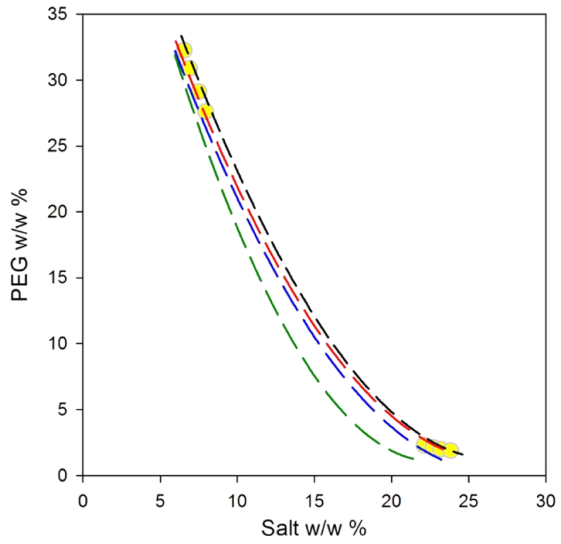

***Figure* 8.** Liquid-liquid equilibrium of the system (PEG 3000 + tri-potassium citrate + water) at pH=8.33, experimental results ●, predictions with, the modified UNIQUAC-FV model – –, Virial-(M & B) – –, extended UNIQUAC model – – and UNIFAC model – –.

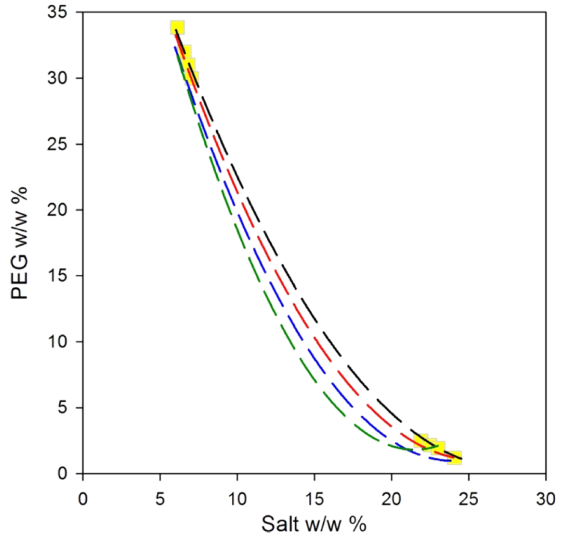

***Figure* 9.** Liquid-liquid equilibrium of the system (PEG 3000 + tri-potassium citrate + water) at pH=9.60, experimental results ■, predictions with, the modified UNIQUAC-FV model – –, Virial-(M & B) – –, extended UNIQUAC model – – and UNIFAC model – –.

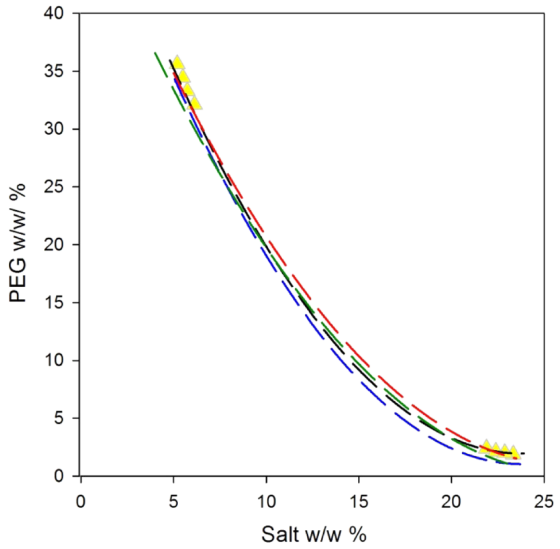

***Figure* 10.** Liquid-liquid equilibrium of the system (PEG 3000 + tri-potassium citrate + water) at pH=10.52, experimental results ▲, predictions with, the modified UNIQUAC-FV model – –, Virial-(M & B) – –, extended UNIQUAC model – – and UNIFAC model – –.

experimental binodal data were satisfactorily correlated with the Merchuk equation and the tie-line compositions were fitted to both the Othmer-Tobias and Bancroft equations. Furthermore, the models could accurately reproduce the experimental data as the data were correlated with the extended UNIQUAC, UNIFAC, Virial-(Mobalegholeslam & Bakhshi) and modified UNIQUAC-FV models to determine the activity coefficient. The better fit was observed in Binodal data in PH = 10.52 by the models. The findings of the three thermodynamics models were adequate and acceptable, in that the obtained binary interaction parameters can be employed for prediction of phase behavior in the investigated quaternary system.

Accknowledgements. The authors would like to thank the anonymous reviewers and the editor for their insightful comments and suggestions. Publication cost of this paper was supported by the Korean Chemical Society.

Supporting Information. Additional supporting information is available in the online version of this article.

REFERENCES

1. Albertsson, P. A. *Partition of Cell Particles and Macromolecules*, John Wiley & Sons: New York, U.S.A., 1986; Vol. 6, p 258.
2. Vernau, J.; Kula, M. R. *Biotechnol. Appl. Biochem*. **1990**, *12*, 397.
3. Sadegh, R. I.; Ziamajidi, F. *Fluid Phase Equilib*. **2007**, *255*, 46.
4. Zafarani-Moattar, M. T.; Hosseinpour-Hashemi, V. *J. Chem. Thermodynamics* **2012**, *48*, 75.
5. Zafarani-Moattar, M. T.; Hamidi, A. A. *J. Chem. Eng. Data* **2003**, *48*, 262.
6. Jayapal, M.; Regupathi, I.; Murugesan, T. *J. Chem. Eng. Data* **2007**, *52*, 56.
7. Pirdashti, M.; Movagharnejad, K.; Rostami, A. A.; Akbarpour, P.; Ketabi, M. *J. Chem. Eng. Data* **2015**, *60*, 3423.
8. Baskir, J. A., Hatton, T. A.; Suter, U. W. *J. Phys. Chem*. **1989**, *93*, 2111.
9. Renon, H.; Prausnitz, J. M. *AIChE* **1968**, *14*, 135.
10. Abrams, D. S.; Prausnitz, J. M. *AIChE* **1975**, *21*, 116.
11. Wilson, G. M. *J. Am. Chem. Soc*. **1964**, *86*, 127.
12. Haghtalab, A.; Joda, M. *Fluid Phase Equilib*. **2009**, *278*, 20.
13. Haghtalab, A.; Mokhtarani, B. *Fluid Phase Equilib*. **2004**, *215*, 151.
14. Xu, X.; Madeira, P. P.; Teixeira, J. A.; Macedo, E. A. *Fluid Phase Equilib*. **2003**, *213*, 53.
15. Sadeghi, R. *J. Chem. Thermodyn*. **2005**, *37*, 55.
16. McMillan, W. G.; Mayer, J. E. *J. Chem. Phys*. **1945**, *13*, 276.
17. Hill, T. L. *J. Chem. Phys*. **1959**, *30*, 93.
18. Haghtalab, A.; Mokhtarani, B.; Maurer, G. *J. Chem. Eng Data* **2003**, *48*, 1170.
19. Perez, B.; Malpiedi, L. P.; Tubío, G.; Nerli, B.; Filho, P. A. P. *J. Chem. Thermodyn*. **2013**, *56*, 136.
20. Pirdashti, M.; Movagharnejad, K.; Mobalegholeslam, P.; Pirdashti, H. *Fluid Phase Equilib*. **2016**, *427*, 460.
21. Hatti-Kaul, R. *Methods in Biotechnology: Aqueous Two-Phase Systems: Methods and Protocols*, Humana Press Inc.: NJ Totowa, 2000; Vol. 1, p 15.
22. Pirdashti, M.; Movagharnejad, K.; Rostami, A. A.; Bakhshi, H.; Mobalegholeslam, P. *Fluid Phase Equilib*. **2016**, *417*, 29.
23. Paksoy, H. Ö.; Örnektekin, S.; Balcl, B.; Demirel, Y. *Thermochimica Acta*. **1996**, *287*, 235.
24. Pirdashti, M.; Movagharnejad, K.; Mobalegholeslam, P.; Pirdashti, H. *Fluid Phase Equilib*. **2016**, *427*, 460.
25. Mobalegholeslam, P.; Bakhshi, H. *J. Solution Chem*. **2016**, *45*, 1826.
26. Ninni, L.; Camargo, M. S.; Meirelles, A. J. A. *Thermochim. Acta*, **1999**, *328*, 169.
27. Sadeghi, R.; Ziamajidi, F. *Fluid Phase Equilib*. **2007**, *255*, 46.
28. de Lemos, L. R.; da Rocha Patrício, P.; Rodrigues, G. D.; de Carvalho, R. M. M.; da Silva, M. C. H.; da Silva, L. H. M. *Fluid Phase Equilib*. **2011**, *305*, 19.
29. de Andrade, V. M.; Rodrigues, G. D.; de Carvalho, R. M. M.; da Silva, L. H. M.; da Silva, M. C. H. *Chem. Eng. J.* **2011**, *171*, 9.
30. Merchuk, J. C.; Andrews, B. A.; Asenjo, J. A. *J. Chromatogr.* **1998**, *711*, 285.
31. Porto, T. S.; Pessôa-Filho, P. A.; Neto, B. B.; Filho, J. L. L.; Converti, A.; Porto, A. L. F.; Pessoa, A. Jr. *J. Ind. Microbiol. Biotechnol*, **2007**, *34*, 547.
32. Shahbazinasab, M. K.; Rahimpour, F. *J. Chem. Eng. Data* **2012**, *57*, 1867.
33. Costa, A. R. D.; Coimbra, J. S. D. R.; Ferreira, L. A.; Marcos, J. C.; Santos, I. J. B.; Marleny, D. A.; Saldaña, M. D. A.; Teixeira, J. A. C. *Food Bioprod. Process*. **2015**, *95*, 118.
34. Perumalsamy, M.; Murugesan, T. *J. Chem. Eng. Data* **2009**, *54*, 1359.